ALUMINIUM INDUCED CRYSTALLIZATION OF HYDROGENATED AMORPHOUS SILICON THIN FILMS

BY

LEBOGANG KOTSEDI

A thesis submitted in partial fulfillment of the requirements for the degree of Magister Scientiae in the Department of Physics, University of the Western Cape.

UNIVERSITY of the
WESTERN CAPE

Promoter: Prof. D. Knoesen, University of the Western Cape

Co-promoter: Prof. R. Madjoe, University of the Western Cape

DECEMBER 2005

http://etd.uwc.ac.za/

DECLARATION

I declare that

"ALUMINIUM INDUCED CRYSTALLIZATION OF HYDROGENATED AMORPHOUS SILICON THIN FILMS"

is my own work and that all the sources used or quoted have been indicated and acknowledged by means of complete references.

UNIVERSITY of the WESTERN CAPE

________________________ ________________________

Lebogang Kotsedi **Date**

http://etd.uwc.ac.za/

ABSTRACT

"ALUMINIUM INDUCED CRYSTALLIZATION OF HYDROGENATED AMORPHOUS SILICON THIN FILMS"

Lebogang Kotsedi

M.Sc thesis, Department of Physics, University of the Western Cape

This study was carried out to crystallize hydrogenated amorphous silicon (a-Si:H) thin films using the aluminium induced crystallization (AIC) technique. This was done to investigate whether is there any lateral crystallization of the a-Si:H thin film away from the aluminium covered surface of the film.

The hot wire chemical vapour deposition system (HWCVD) was used to deposit hydrogenated amorphous silicon thin films (a-Si:H) on Corning glass 7059 substrates. The substrate temperature was kept at 300°C while the filament temperature was 1600°C during the deposition.

The aluminium top layer was deposited at room temperature using the electron beam evaporator. The aluminium deposited, only partially covered the sample, this was done to investigate whether lateral crystallization of the uncovered part will take place.

Samples were then annealed at 450°C for times ranging from 30 to 150 minutes in incremental steps of 30 minutes. A temperature series of annealings at 100°C, 150°C, 200°C, 300°C and 350°C for 60 minutes were also performed. Energy Dispersive Spectroscopy (EDS) was used for elemental identification after annealing. Rutherford Backscattering Spectrometry was used for the depth profiling of the diffused species. X-ray diffraction (XRD) technique was used for crystallization studies on the aluminium covered side, transmission electron microscopy (TEM) was used to study

http://etd.uwc.ac.za/

lateral crystallization and diffraction patterns of crystallized part were taken using selected area diffraction (SAD).

The Aluminium that diffused into the a-Si:H film acted as the nucleation sites for the growth of poly c-Si. XRD results from the aluminium covered side showed that the film was crystallized after annealing at 450°C for all annealing times. TEM and SAD also confirmed that the original a-Si:H film covered by aluminium was crystallized and from the TEM micrograph lateral crystallization was also observed.

http://etd.uwc.ac.za/

ACKNOWLEDGEMENTS

To my Redeemer, Jesus Christ.

I would like to express my gratitude to the following distinguished people, without whose assistance, advice, guidance and friendship this thesis would not have been possible.

Prof. Dirk Knoesen of the Physics Department of the University of the Western Cape (UWC), who is the promoter of this research, for his exceptional expertise, guidance offered especially during the TEM sample preparation and analysis and also for the stimulating and fruitful discussions.

Prof. Reginalt Madjoe, of the Physics Department of the University of the Western Cape (UWC), for his support during the e-gun deposition at iThemba LABS, and fruitful discussion during oral presentations.

Mr. Theophillus Muller, of the Physics Department of UWC, for his continous help since the beginning of this research and for his friendship and especially for giving me rides to iThemba LABS.

Dr. Chris Theron of iThemba Materials Research Group for his fruitful discussions and teaching me some RUMP manipulations.

Dr. Terrence Marais of the Physics Department of UWC, for his continuous support, interest in my work and for his big heart.

Dr. Remy Bucher of iThemba LABS Materials Research Group, for helping me with the XRD measurements and for the fruitful discussions.

Mr Tshepo Ntsoane of iThemba LABS Materials Research Group, for his fruitful discussions and assistance during XRD experiments.

UNIVERSITY of the
WESTERN CAPE

http://etd.uwc.ac.za/

Mr Gabriel Pitsoane of iThemba LABS Materials Research Group, for his assistance during RBS experiments.

Mr Phillip Sechogela of iThemba LABS Materials Research Group, for his assistance during the RBS experiments and RUMP simulations.

To the Hector Peterson Christian group for their continuous support and prayers during trying times. Thank you guys.

Drs W. Pienaar, C. Pienaar, for their encouraging sermons, teachings, dedication to the student ministry and their hard work.

Pastor Mogosi for her motherly love, prayers, hospitality and sincere interest in my well being.

My sister Boipelo 'Davi', Motlalepule and Motsalo for looking after me since the beginning of my academic work and for their continuous support.

Citi for his friendship and advises.

My mother, Mathlodi, for her 100% support, love encouragement and patience during studies.

NRF, iThemba LABS and Physics Department at UWC, for financial assistance during the course of this study.

All those who were of assistance in any form of ways during this research work.

My Creator and my Lord Jesus Christ.

UNIVERSITY of the
WESTERN CAPE

http://etd.uwc.ac.za/

CONTENTS

Title Page .... (i)
Declaration .... (ii)
Abstract .... (iii)
Acknowledgements .... (v)
Contents.......... (vii)
Keywords .... (ix)
List of abbreviation .... (x)
Physical Constants .... (xii)

Chapter 1: INTRODUCTION

1.1 Solar Energy 1
1.2 Silicon Technology 2
1.3 Amorphous Silicon 4
1.3.1 Hydrogenated amorphous silicon 4
1.4 Crystallization of hydrogenated amorphous silicon 4
1.4.1 Metal induced crystallization 5
1.5 Aim and Outline 7

Chapter 2: EXPERIMENTAL METHODS

2.1 Deposition of a-Si:H using HWCVD 8
2.1.1 Reaction chamber 8
2.1.2 Deposition conditions 9
2.1.3 E-gun evaporator 11
2.14 Sample layout 12
2.2Thickness measurements 12
2.3 Heat treatment 14
2.4 X-ray diffraction (XRD) 15
2.5 Rutherford Backscattering Spectrometry (RBS).......... 17
2.6 Transmission Electron Microscopy (TEM).......... 20
2.7 Energy Dispersive Spectroscopy 22

http://etd.uwc.ac.za/

Chapter 3: RESULTS

3.1 Introduction 24

3.2 Experimental results 25

3.2.1 Thickness Measurements 25

3.2.2 Energy Dispersive Spectroscopy (EDS).......... 26

3.2.3 Rutherford Backscattering Spectroscopy (RBS) 27

3.2.4 X-ray Diffraction (XRD).......... 30

3.2.5 Transmission Electron Microscopy (TEM) 34

Chapter 4: DISCUSSION

4.1 Introduction 36

4.2 Analysis of results 36

Chapter 5: CONCLUSION

5.1 Conclusion 40

5.2 Suggestion for Future Research 42

REFERENCES

References 43

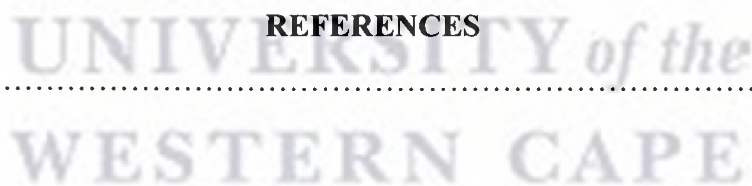

UNIVERSITY of the
WESTERN CAPE

http://etd.uwc.ac.za/

Keywords

ALUMINIUM INDUCED CRYSTALLIZATION OF HYDROGENATED AMORPHOUS SILICON THIN FILMS

Hot-wire chemical vapour deposition (HWCVD)
Hydrogenated amorphous silicon (a-Si:H)
Poly-crystalline silicon (poly c-Si)
Aluminium Induced Crystallization (AIC)
Lateral crystallization
Aluminium thin film
Crystallization
Uncrystallized
Small cracks
Amorphous

http://etd.uwc.ac.za/

LIST OF ABBREVIATIONS

MATERIALS

a-Si : Amorphous silicon

a-Si:H : Hydrogenated amorphous silicon

Poly c-Si : Polycrystalline silicon

c-Si : Single crystalline silicon

μc-Si:H : Hydrogenated microcrystalline silicon

Al : Aluminium

SiH_4 : Silane gas

Ti : Titanium

Cu : Copper

Pd : Palladium

In : Indium

Au : Gold

Ni : Nickel

W : Tungsten

Fe : Iron

DEPOSITION TECHNIQUES

HWCVD : Hot-Wire Chemical Vapour Deposition

E-gun : Electron gun

DEPOSITION PARAMETERS

T_{fil} : Filament temperature

T_{sub} : Substrate temperature

P : Pressure

Sccm : Standard cubic centimeter per minute (flow rate)

$1sccm = V_m^{-1} \times 10^{-6} m^3/60 \sim 7.440 \times 10^{-7}$ mol s^{-1}

http://etd.uwc.ac.za/

ANALYTICAL TECHNIQUES

XRD : X-ray diffraction

SEM : Scanning electron microscopy

EDS : Energy dispersive spectroscopy

TEM : Transmission electron microscopy

RBS : Rutherford backscattering spectrometry

*atoms/cm^2 = 10^{15} atoms/(ρ) × 10^8 = Å

ρ : Element atomic density

Corning glass composition.

Target composition: 49 wt% SiO_2, 10 wt% Al_2O_3, 15 wt% B_2O_3, 25 wt% BaO, 1 wt% As_2O_3. [45]

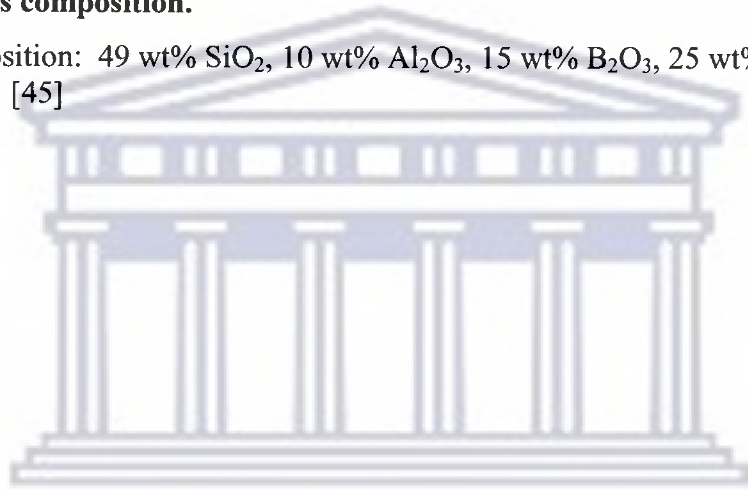
UNIVERSITY of the
WESTERN CAPE

http://etd.uwc.ac.za/

PHYSICAL CONSTANTS

Constant	Symbol	Value
Atomic density of aluminium	ρ_{al}	6.023×10^{22} atoms/cm^3
Atomic density of silicon	ρ_{si}	4.9777×10^{22} atoms/cm^3

http://etd.uwc.ac.za/

CHAPTER 1

INTRODUCTION

1.1 Solar Energy

Solar cell technology has proved to be at the fore-front of solving the problems of present methods of generating electricity. There are various ways of generating electricity from different sources, ranging from nuclear to oil to coal. Some of these methods have proved to be environmentally expensive than the others.

Fossil fuels (coal) are burned in order to generate electricity and during the process carbon dioxide gas is released into the atmosphere. This carbon dioxide gas in turn is trapped into the atmosphere and lead to global warming. Fossil fuel (coal) technology of generating electricity contributes to the escalating amounts of carbon dioxide in the atmosphere. This has proved to be a very expensive approach to make life convenient.

On the other hand nuclear technology of generating electricity has some major shortcomings when it comes to health and environmental safety. It produces radioactive waste that requires very carefully controlled disposal, this radioactive waste have very long half lives and have a higher potential of posing danger to the environment.

Then there are oil and gas technologies of generating electricity that also are harsh to the environment due to the pollution they cause and their contribution to the global warming. These forms of technologies and the others have long term negative effects to our environment and the well being of the eco-system, hence cheaper and safe technologies of generating electricity are being actively searched and researched upon.

The good news is that the same lifestyle of convenience can be maintained, but using environmentally friendly means of generating electricity. This can be achieved by using renewable energies like the sun to produce electricity. The seeds of these ideas

UNIVERSITY of the WESTERN CAPE

http://etd.uwc.ac.za/

were planted by Becquerel whom in his experiments noticed a light-depend voltage between electrodes immersed in an electrolyte. The full understanding of this light-induced phenomenon was attained in the 1940's and the 1950's the first usable solar cell was built [1 – 2].

The free energy from the sun can be converted to electricity, photon energy from the sun is absorbed by the solar cell panel when the photon energy excites the electrons from the valence band to the conduction band, in doing so generating a charge separation that is used in the generation of electricity.

There are many different solid state materials that can be used for the generation of electricity using energy from the sun, these are called photo-voltaic materials (photo meaning sunlight and voltaic from voltage). These materials vary from gallium arsenide to silicon technology. For the purposes of this paper the focus will be on silicon technology.

1.2 SILICON TECHNOLOGY

UNIVERSITY of the
WESTERN CAPE

In the silicon technology various forms of silicon can be used to manufacture photo-voltaic cells for the generation of electricity, namely single crystalline silicon (c-Si), hydrogenated poly-crystalline silicon (poly C-Si), hydrogenated micro-crystalline silicon (μc-Si:H) and hydrogenated amorphous silicon.

Single crystalline silicon solar cell technology has the higher efficiency in the silicon solar cell technology but this comes with some limitations. Large photo-voltaic areas are needed to develop sufficient power from incident sunlight on the panels of the solar cell, but single crystalline silicon solar cells are less efficient in surface area coverage, this is due to its profile from the manufacturing processes. Single crystalline silicon wafers are mostly circular in shape and are too expensive to cut then into a square pattern, hence cannot cover the whole area of the panel. This leaves some

http://etd.uwc.ac.za/

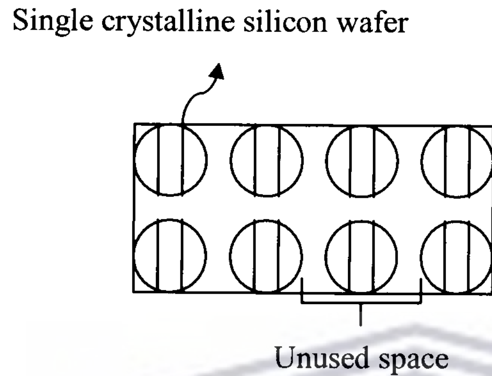

Figure 1.1 Single crystalline silicon solar cell panel.

unused spaces in the panel, when photons fall on that area they are not generating electricity. This shortcoming of single crystalline solar cell can be overcome by using other forms of silicon that can fill the whole panel area so as to utilize maximum incident photon energy.

Micro-crystalline hydrogenated silicon (μc-Si:H) can be deposited as layers covering the whole substrate area hence solving the problem of unused spaces. The deposition of μc-Si:H can be achieved by merely changing the feed gas composition in the HWCVD reaction chamber. Silane and hydrogen gases are used as feed gases for deposition of μc-Si:H, by varying the ratio of these gases a μc-Si:H thin film can be grown on a substrate. Chamber pressure, filament and the substrate temperature are also important parameters to consider when growing μc-Si:H. These μc-Si:H thin films can be used to manufacture solar panels which can fill the panel and have maximum surface area. But a solar cell with both large surface area and better efficiency can be realized by first depositing a-Si:H on a large surface and then crystallizing it to get a hydrogenated poly-crystalline silicon which has a better carrier mobility.

http://etd.uwc.ac.za/

1.3 AMORPHOUS SILICON (a-Si)

Amorphous silicon is a form of silicon that has no long range order but similar short range order to that of c-Si. In this structure the silicon atoms are normally fourfold coordinated. The structural model of a-Si is generally described as a continuous random network, but a fourfold continuous random network is over coordinated because of the presence of too many bonding constrains compared to the number of degree of freedom [3,4]. This result in a-Si having a higher crystallization temperature. To achieve a relax network and hence lower crystallization temperatures the network coordination must be reduced. This can be done by incorporating H atoms into the a-Si network to produce a-Si:H [3,4].

1.3.1 HYDROGENATED AMORPHOUS SILICON (a-Si:H)

Hydrogenated amorphous silicon is a form of silicon that has no atomic long range structural order. The presence of hydrogen atoms helps to improve network coordination by terminating Si bonds and resulting in a less constrained network. Hydrogen atoms again help to electronically passivate the dangling bonds of the a-Si network [3,4]. When the *metal induced crystallization technique* is used to crystallize a-Si:H, lower crystallization temperatures are achieved because of the influence of hydrogen.[5]

A-Si:H thin films were deposited by a HWCVD technique using Silane(SiH_4) as a source gases. Good quality a-Si:H thin films were deposited on Corning 7059 glass, these thin films of a-Si:H were subsequently crystallized using the *metal (aluminium) induced crystallization technique.*

1.4 Crystallization of Hydrogenated Amorphous Silicon

Hydrogenated amorphous silicon can be crystallized using various methods, like solid phase crystallization [6], and excimer laser crystallization [7]. Solid phase

http://etd.uwc.ac.za/

crystallization is a process whereby hydrogenated amorphous silicon is annealed for approximately 30 hours at a temperature of 600°C in a vacuum, this is an expensive process because of it high thermal budget and processing time. While on the other hand crystallization by laser annealing has some shortcomings, like uniformity over large area and is also expensive due to the technology needed for the process, hence new techniques of crystallizing a-Si:H have been researched.

1.4.1 Metal Induced Crystallization

In the recent years it was discovered that when a metal layer is in contact with a-Si:H thin films in the annealing furnace, a-Si:H tends to crystallize at lower temperatures compared to when they are not covered. It was concluded that the presence of the metal induces crystallization of a-Si:H films at lower temperatures.

Metal induced crystallization is a technique that has the advantage of having short processing time and lower thermal annealing temperatures. In this process a-Si:H films covered by a thin layer of metal are annealed under vacuum or under ambient of choice, as result of the presence of the metal layer the a-Si:H thin film crystallizes faster and at lower temperatures than the solid phase crystallization [8]. The commonly used metals are Al, Ti, Cu, Pd, Au, Fe, In, W, Sn and Ni [9-27]. But from this group of metals Ni, W, Ti, Cu and Fe tend to form silicides at temperatures at which crystallization occurs which is undesirable [28-33]. On the other hand Al, Au, In and Pd are such that their eutectic temperature in the Si/Al, Si/Au, Si/In and Si/Pd systems are higher than the crystallization temperature induced by the presence of these metals which makes them metals of choice. Due to the abundance and affordability of aluminium relative to palladium (Pd) and other metals, aluminium was chosen as a metal of choice for this research project. The advantage of using

UNIVERSITY of the WESTERN CAPE
http://etd.uwc.ac.za/

metal induced crystallization is that cheap substrates can be used for depositing a-Si:H thin films and crystallize them since lower temperatures are used, temperatures that are far from softening or glass transition temperatures of most cheap substrates. This in turn gives a platform to produce affordable solar cell panels and electronic devices using cheap substrate materials. The resulting hydrogenated poly-crystalline silicon can also be used as a seed for epitaxial thickening of the poly-crystalline layer for other various applications. This will be a good cost cutting exercise since it is reported that up to half the cost of the semiconducting device is on crystalline silicon [34].

A question arises as to whether a-Si:H thin films half covered by aluminium layer will induce lateral crystallization of the aluminium overlaid part of the a-Si:H film to the uncovered part. If this is the case then a reduced surface covering in the metal would be sufficient to crystallize the complete a-Si:H thin film.

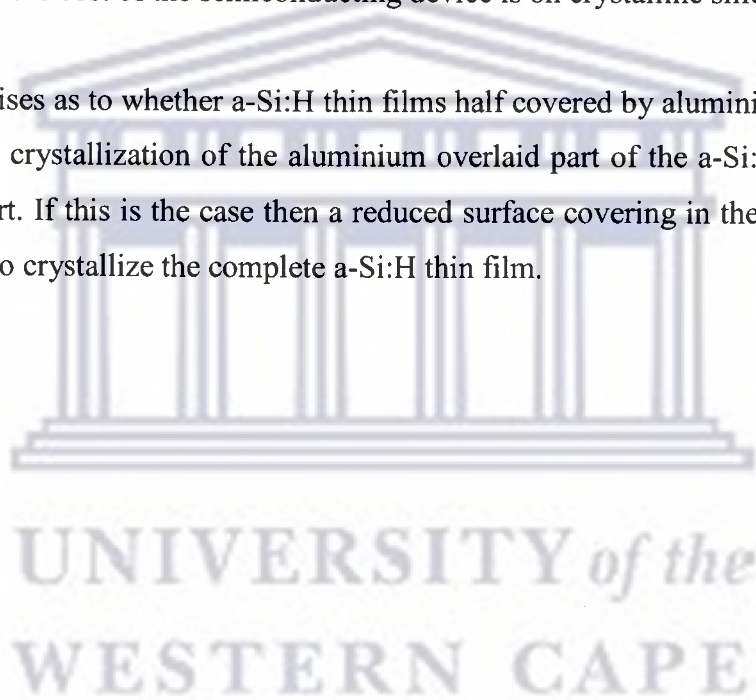
UNIVERSITY of the
WESTERN CAPE

http://etd.uwc.ac.za/

1.5 Aim and Outlines

In this investigation the aim is to crystallize a-Si:H thin films using aluminium as a metal of choice. Thin films of a-Si:H were deposited on corning glass 7059 substrate using Hot-Wire Chemical Vapour Deposition (HWCVD). Silane gas was used as the source gas for the deposition of a-Si:H thin films. The conditions used to deposit these a-Si:H films were the best ones to produce a quality a-Si:H thin film based on extensive research of the best conditions for the deposition of these films.

The deposited substrate were then cut into 1cm × 1cm squares and a thin layer of aluminium was deposited on the a-Si:H thin films, only half covering the sample. This was done to test and measure lateral growth range in the a-Si:H layer away from the metal edge. These were annealed and analyzed using various analytical techniques, the following were employed: XRD, TEM, RBS, EDS and Dektak Profilometer was also used. These analytical techniques are explained in chapter two.

The results of the above mentioned analytical techniques are stated in chapter three and in chapter four the discussion of the observations is made, and some conclusions are made based on literature and hypotheses.

UNIVERSITY of the
WESTERN CAPE

http://etd.uwc.ac.za/

CHAPTER 2

EXPERIMENTAL METHODS

2.1 DEPOSITION OF HYDROGENATED AMORPHOUS SILICON USING HWCVD.

The hydrogenated amorphous silicon thin films prepared for this study were deposited on Corning 7059 glass. This Corning glass is a highly important optical substrate material that can survive the deposition conditions necessary for the deposition of a-Si:H thin films and the annealing processes. The optical properties of Corning glass allows transmission of UV spectrum if UV/ visible spectrometer that is used to characterize the optical properties of the deposited a-Si:H films is to be used. Hot Wire Chemical Vapour Deposition (HWCVD) technique was chosen to grow these thin films of a-Si:H, this technique was chosen because of its low hydrogen content a-Si:H films and good growth rate.

The reaction chamber used for the deposition of a-Si:H is an MV Hot Wire CVD, this machine is a single chamber system that can reach ultra-high vacuum pressure in the reaction chamber. These ultra-high vacuums are achieved by using a turbo molecular pump that is backed by a Leybold D40B rotary vane pump. Adjacent to this reaction chamber is a loading chamber which also can be evacuated, this loading chamber is separated from the reaction chamber by a valve gate. The samples are first loaded onto a sample holder in the loading chamber and then inserted into the reaction chamber for deposition.

2.1.1 REACTION CHAMBER

In the reaction chamber there is a tantalum filament which can be resistively heated to required temperatures to deposit quality a-Si:H films, the filament

http://etd.uwc.ac.za/

temperature is monitored by a Foster optical pyrometer through a window in the reaction chamber. Also there is a heater at the top of the reaction chamber, to heat the substrate to the desired temperatures, and the temperature of the substrate is in turn monitored by a K-type thermocouple. Just below the substrate holder position in the reaction chamber there is a shutter that can be placed over the substrate to prevent any further growth of the film.

The flow rates of the gases pumped into the reaction chamber are measured using gas flow meters which can be set to any desired flow rate. When the desired film thickness has been grown the gas flow is stopped, and the reaction chamber is evacuated before the removal of the sample to the load lock. The sample is then left in load lock to cool down to room temperature.

2.1.2 DEPOSITION CONDITIONS

In order to grow a thin film of a-Si:H using HWCVD silane gas is used as a source, or if desired the silane gas can be diluted with hydrogen gas. Silane gas decomposes when it passes over the resistively heated tantalum filament, this results in hydrogenated amorphous silicon film growing on the heated substrate above the hot filament in the reaction chamber.

Table 2.1 shows the deposition conditions that were used to grow a-Si:H films. These conditions were chosen such that the grown films have low hydrogen content and the material is dense.

Table1 Deposition conditions

	H_2	**SiH_4**	**Flow rate(gases)**	**Sub_{temp}**	**$Filam_{temp}$**	**Pressure**	**Duration**
Corning glass	0 sccm	30 sccm	30 sccm	300°C	1600°C	30μbar	8.5 minutes

http://etd.uwc.ac.za/

A 10 cm X 10 cm Corning 7059 glass plate 1mm thick was the substrate of choice for the deposition. These were cleaned firstly in acetone followed by spray washing them by methanol and left to dry. This glass was then loaded onto a sample holder on the HWCVD, then placed in the loading chamber for the first deposition.

For the deposition, the silane gas flow rate was set at 30 sccm and the tantalum filament was resistively heated to 1600°C. These conditions were measured using gas flow rate monitor and the Foster optical pyrometer. The substrate heater was at 300°C and the reaction chamber vacuum pressure was controlled at 30 μbar. Lastly the substrate-filament distance was always fixed at 33 mm.

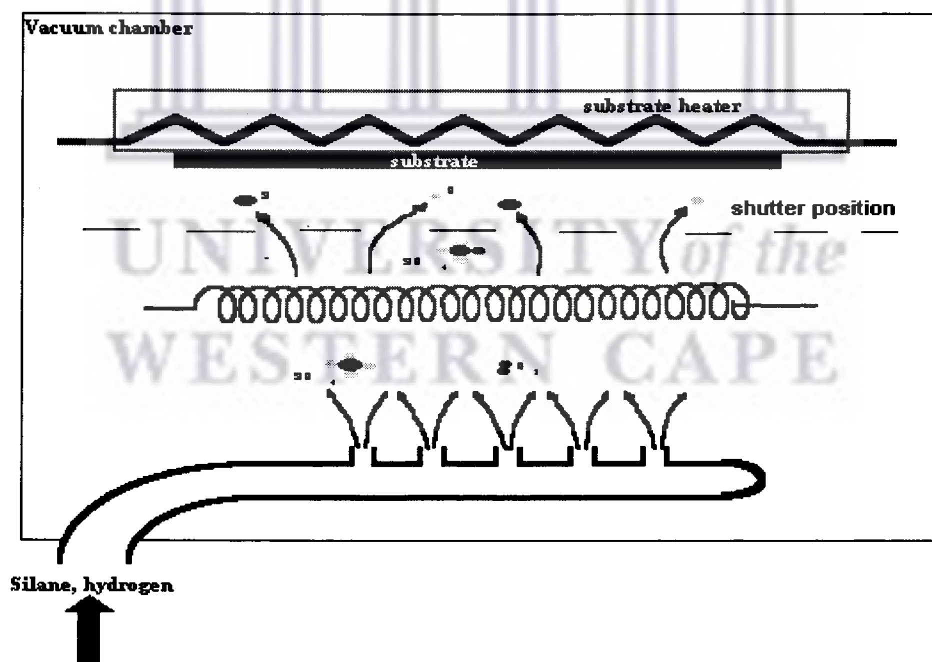

Figure 2.1 Schematic of the Hot-wire CVD reaction chamber.

http://etd.uwc.ac.za/

2.1.3 E-Gun EVAPORATOR

Electron gun evaporation is a technique that uses thermo ionic electrons ejected from a resistively heated tungsten filament to heat up a metal until it evaporates. This deposition is usually done under high vacuum pressures and at room temperature. The deposition chamber must be cleaned well before the deposition is done to avoid impurities from previous depositions being incorporated into the deposited film.

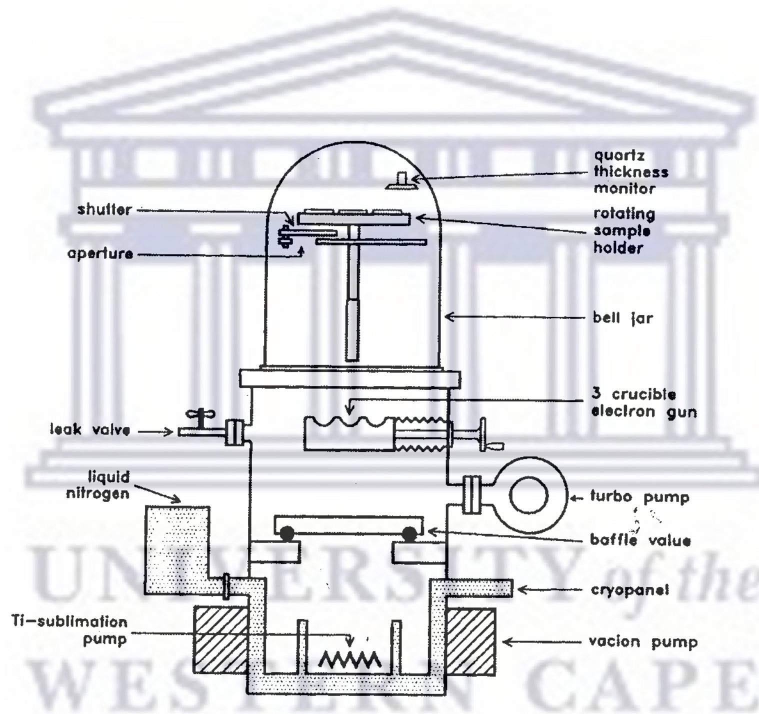

Figure 2.2 Schematic representation of e-gun evaporator.

The samples to be covered by aluminium were placed on the sample holder and aluminium balls of 99.999% purity were put into the crucibles. The e-gun chamber used can reach high vacuum pressures, pumped by turbo molecular and Titanium sublimation pump to a vacuum presssure of 10^{-7}mbar before the deposition of the element. The deposition rate and the thickness of the deposited film were monitored by the quartz crystal thickness monitor.

http://etd.uwc.ac.za/

2.1.4 Sample Layout

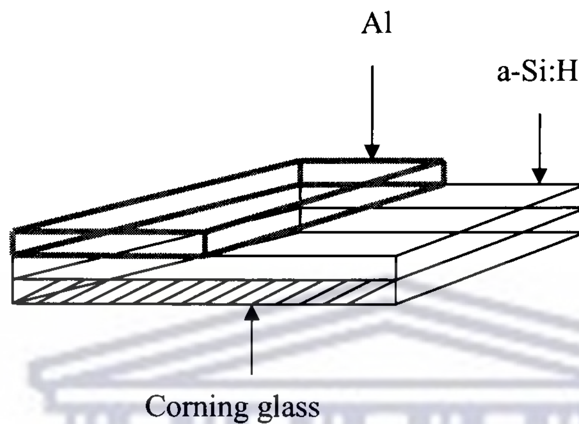

Figure 2.3 Sample layout.

The samples were left in the chamber for an hour to cool down before taking them out. Figure 2.3 shows a 1 cm × 1 cm sample layout after the deposition of a-Si:H and aluminium thin films on the corning glass substrate. As it is shown in figure 2.3 above the a-Si:H thin film is only half covered by aluminium, the thickness of aluminium was determined using Dektak Profilometer.

2.2 Thickness Measurement using Profilometry

Dektak Profilometer was used for thickness determination of the deposited aluminium, the profilometer measures the thickness step height difference between the films of a-Si:H and aluminium using a very sensitive stylus for contact. The graph shown in figure 2.4 is the representation of the step height difference between these two thin films, this step height difference gives the thickness of the aluminium layer.

Dektak profilometer has a wide range of analytical functions, as it can be used for roughness, waviness, step height and geometrical measurements. The profilometer

http://etd.uwc.ac.za/

makes measurements electronically by moving the high precision stage with the sample beneath a diamond tipped stylus according to a user programmed scan length,

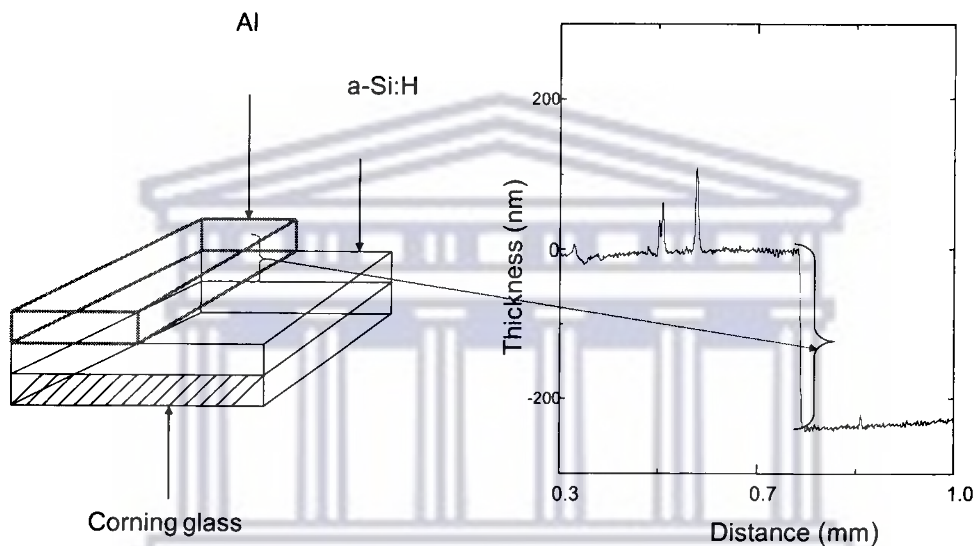

Figure 2.4 Schematic diagram of Dektak measurement.

UNIVERSITY of the
WESTERN CAPE

speed and stylus force. The stylus is mechanically coupled to the core of a Linear Variable Differential Transformer (LVDT). As the stage moves the sample, the stylus rides over the sample surface. The surface variations cause the stylus to be translated vertically. Electrical signals corresponding to the stylus movement are produced as the core position of the LVDT changes. The LVDT scale is an AC reference signal proportional to the position change, which in turn is conditioned and converted to a digital format through a high precision integrating analog-to-digital converter. The digitized signals from printing a single scan are stored in computer memory for display, manipulation, measurement, and printing. [35]

http://etd.uwc.ac.za/

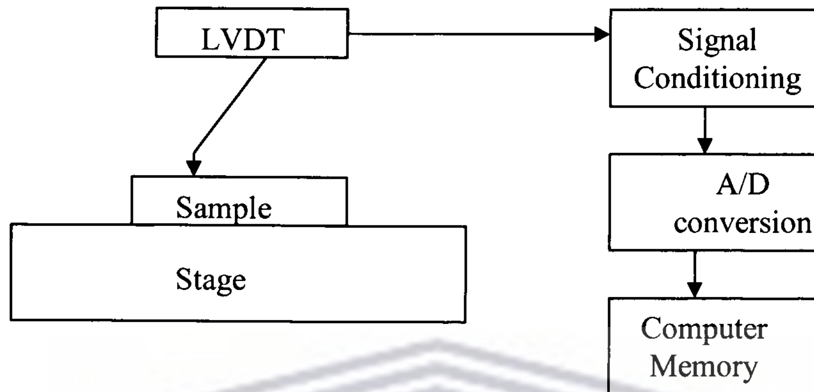

Figure 2.5 Block diagram of Dektak

2.3 Heat Treatment

The samples were heated under vacuum using a multi-sample carousel system. The furnace was evacuated to pressures of 10^{-7}mbar before the samples were annealed individually. Below is the table of the annealing furnace conditions that were used during the experiment.

UNIVERSITY of the
WESTERN CAPE

Table 2: Temperature series of annealed samples

	Glass/a-Si:H/Al
Temperature (°C)	100°C
	150 °C
	200 °C
	300 °C
	350 °C

http://etd.uwc.ac.za/

For the temperature series, annealing was carried out for 60 minutes under vacuum, and for time series the temperature was set at 450°C for all samples also carried under vacuum

Table 3: Time series of the annealed samples

	Glass/a-Si:H/Al
Duration	30 min
	60 min
	90 min
	120 min
	150 min

After the annealing process was finished, the samples were left in the carousel for an hour for them to cool down before removal. The vacuum was broken using high purity nitrogen gas after the samples have cooled down.

2.4 X-Ray Diffraction (XRD)

X-rays are electromagnetic radiation with the wavelength in the range of 0.5 – 2.5 Å. The short wavelengths of x-rays are good probes to study atomic structure in solids. X-rays can give information as to whether the sample is crystalline or amorphous, and if crystalline also their crystallographic orientation. This information is extracted from the diffracted x-rays spectrum.

$CuK\alpha_1$ radiation was used to study the microstructure of all the samples. These $CuK\alpha_1$ radiation are produced when electrons from the heating filament are accelerated to a very high speed by a very high voltage in the range of few kilo-voltages. When these accelerated electrons hit the copper metal target the electrons from the metal are ejected, then the electrons from higher energy states fill the

http://etd.uwc.ac.za/

vacancies of the ejected electrons. In the process the excessive energy is released in the form of x-rays.

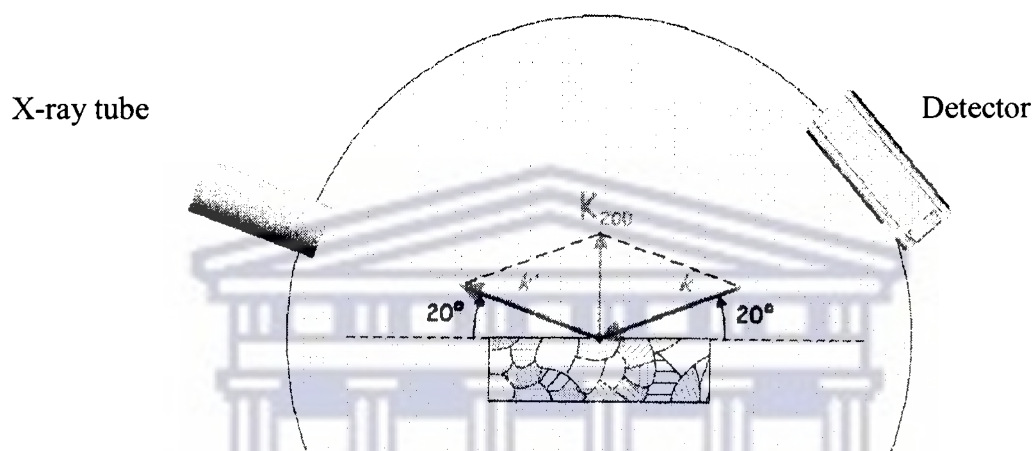

Fig 2.6 Schematics of the experimental setup.

During the process of producing x-rays, x-rays of different wavelength are emitted from the target material. But for the diffraction purposes it is essential to work with radiation which is monochromatic as possible. The intensities of undesirable components such as Kβ- radiation can be attenuated relatively to the Kα-radiation by passing the beam through a filter. The filters are materials that are designed in such a way that the K absorption edge lies between the Kα and the Kβ wavelength of the copper target metal. When the x-ray radiation passes through such a filter the Kβ component of the radiation will be absorbed much stronger than the Kα component.

The intensity ratio of the Kβ to Kα can be controlled by the thickness of the filter material, the thicker the filter the lower the ratio of intensity of Kβ to Kα. The x-rays that are emitted from the x-ray tube impinged the sample, some x-rays are transmitted and some diffracted, the diffracted x-rays are collected by the detector and analyzed by the digital data acquisition system. Diffraction peaks are then obtained. A θ to 2θ

UNIVERSITY of the
WESTERN CAPE

http://etd.uwc.ac.za/

D8 Advanced Bruker x-ray diffraction (XRD) machine was used to analyze the microstructure of the samples. Below is typical XRD spectra of annealed a-Si:H covered with a layer of aluminium, the notation on top of the diffraction peaks is the preferred orientation of the crystallites in the crystallized silicon films.

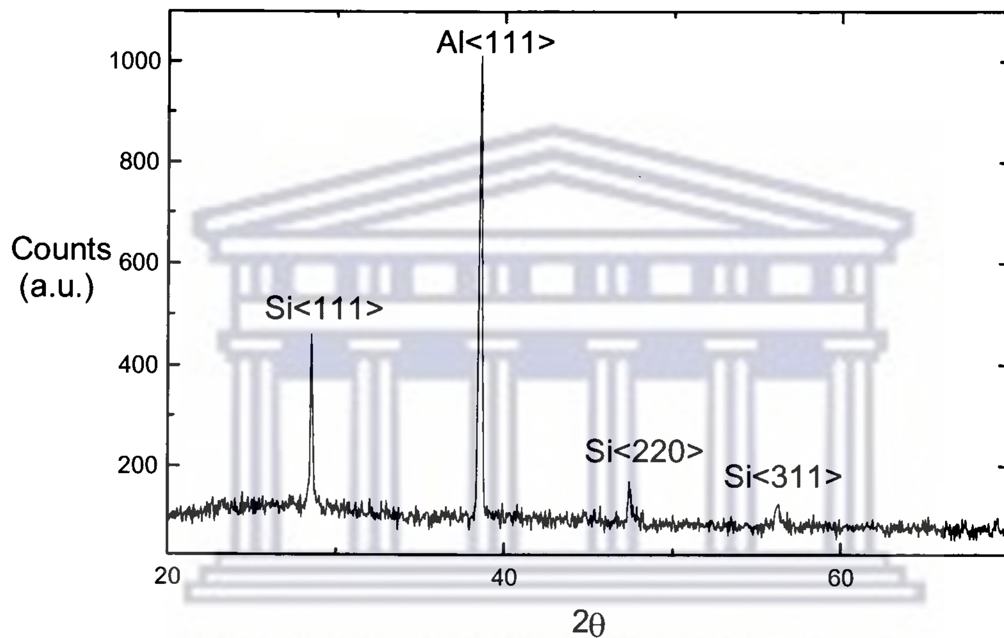

Figure 2.7 XRD Spectra

UNIVERSITY of the WESTERN CAPE

2.5 Rutherford Backscattering Spectrometry (RBS)

Rutherford Backscattering Spectrometry is a non-destructive technique that is used in the depth profiling of the samples. This technique has proved to be important in studying the diffusion of the aluminium into a-Si:H and for thickness determination of the diffused aluminium.

Rutherford Backscattering spectroscopy is an analytical technique that uses high energy light particles (H^+, He^{2+}) to penetrate the sample, the particles are then gradually slowed down as they collide with the atoms in the structure and experience

http://etd.uwc.ac.za/

repulsive force from the nucleus of the atoms. Some of these particles are eventually backscattered due to the repulsive forces of the nucleus, these backscattered particles are then collected by the semiconductor nuclear particle detector for digital processing.

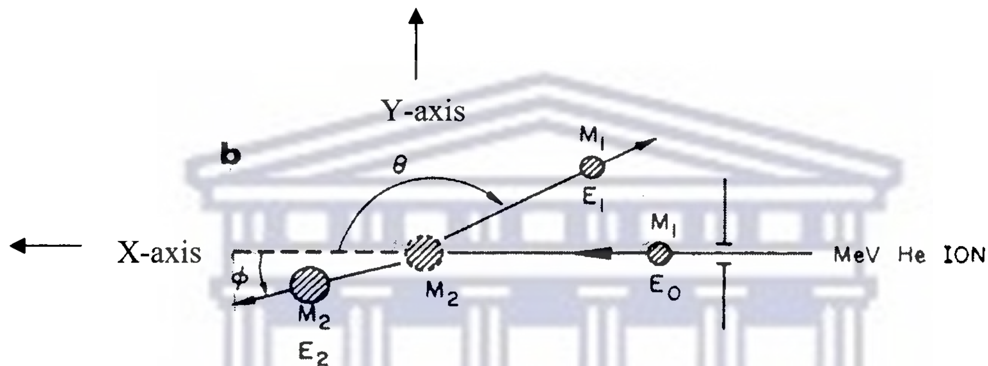

Fig 2.8 Schematics of the experimental setup for Rutherford backscattering.

In Rutherford backscattering spectrometry technique, a monogenetic particles in the incident beam collide with a target atom's nucleus and as a result scatters backwards into the detector. This solid state detector measures the energies of the particles backscattered during the collision with the atoms. During the collision some energy is transferred from the incident particle to the stationary target atom, the reduction in energy of the incident particle is dependent on the masses of the incident and target atom.

The energy transfer between two particles can be solved by applying conservation of energy and momentum. For an incident particle of mass M_1, the values of the velocity and energy are used in form of kinetic energy $E_o = ½ M_1 v^2$. Then after the collision between the incident beam and the stationary atom, the values of the velocities determined by the scattering angle θ and the recoil angle ϕ. The schematics of the experimental setup are given in figure 2.8.

http://etd.uwc.ac.za/

$V_{incident\ particle}$ and $V_{target\ atom}$ and the energies $E_{backscattered\ particle}$ and $E_{target\ atom}$ are determined by the scattering angle θ and the recoil angle φ. The schematics of the experimental setup are given in figure 2.8.

The conservation of energy and momentum in the x, and y coordinates are given the following equations.

Energy :	$\frac{1}{2} M_1 v^2 = \frac{1}{2} M_1 v_1^2 + M_2 v_2^2$,
Momentum in x:	$M_1 v = M_1 v_1 \cos\theta + M_2 v_2 \cos\phi$,
Momentum in y:	$0 = M_1 v_1 \sin\theta - M_2 v_2 \sin\phi$.

From this equations the kinematic factor ($K = E_1/E_o$) can be derived [37]. The kinematic factor is shown to be only mass dependent with the relation given by the equation

$$\frac{E_2}{E_0} = \frac{4 M_1 M_2}{(M_1 + M_2)^2} \cos^2 \phi$$

The samples to be analyzed were mounted onto the RBS sample ladder and loaded into the chamber. The chamber was then evacuated to the pressure of 10^{-5}Pa, then the samples were bombarded with He^{2+} ions. The energies of the backscattered particles were collected by the solid state detector and digitally analyzed and stored in the PC. The XRump program was used for simulation of the spectra. Figure 2.9 shows a typical RBS spectra of as-deposited a-Si:H with a thin layer of aluminium on top and Corning glass as a substrate.

http://etd.uwc.ac.za/

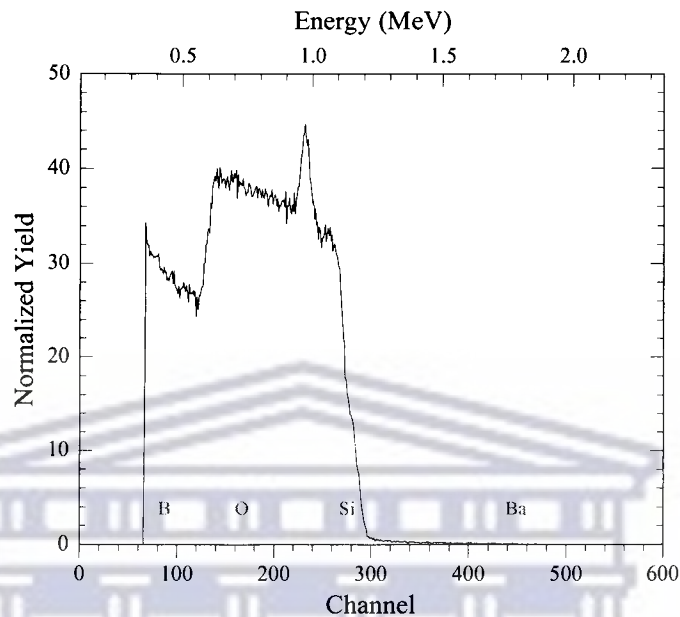

Figure 2.9 RBS Spectra of annealed glass/a-Si:H/Al.

Element shown on the RBS spectrum are energies for the elements when they are at the surface.

UNIVERSITY of the
WESTERN CAPE

2.6 TRANSMISSION ELECTRON MICROSCOPY (TEM)

Transmission electron microscopy was used to study the lateral crystallization of the samples of a-Si:H due to the crystallization of the aluminium covered part of the sample.

TEM is used to probe the internal structure of materials giving access to the micro-structural details of the material. It achieves this by accelerating electrons through a potential difference of 200 kV, at this potential difference the electrons have a wavelength of 0.025 nm hence are good agents for study of the material at a nanometer scale.

http://etd.uwc.ac.za/

In a TEM the beam of electrons are emitted from a hot tungsten filament, these electrons are accelerated by a high voltage of 200 kV, the beam is then passed through a series of lenses. First condensing lenses then the objective lens and lastly the beam is passed through the projection lenses.

The condenser lenses are used to demagnify the beam emitted by the e-gun and to control its diameter and convergence angle as it impinge on the sample, this helps to control the area to be imaged. Just below the condenser lenses is the sample holder which can be moved in the x, y, and z directions. Then there are an objective lenses which forms the first image which is enlarged by the projector lenses and then displayed on the screen. The first projector lens is focused on the image plane of the objective lens and the magnification of the first image is controlled by the strength of the remaining projector lens. The objective aperture to be inserted in the column of the focal plane is there to define the angle of scattered electrons which travel down the column plane and form an image [37].

Samples for the TEM analysis were prepared by sandwiching the specimen of interest between thin strips of silicon wafer, followed by thinning using the mechanical grinding to approximately 50μm thickness. The final thinning process was done by ion milling apparatus (Ion Tech model) using a beam of energetic Argon ions. The samples were milled at angles between 8° and 10° while the sample was rotated to avoid ridges being formed at the surface.

The prepared samples were then probed in the TEM to search for any crystallinity. Diffraction patterns were taken to identify crystalline and the amorphous regions at the laterally crystallized part of the analyzed sample.

http://etd.uwc.ac.za/

2.7 ENERGY DISPERSIVE SPECTROSCOPY (EDS)

EDS was performed on the sample for elemental identification, to investigate whether there was any diffusion of aluminium beyond the edge of the aluminium half covering the a-Si:H film. Scanning electron microscopy (SEM) was used in the EDS mode for elemental identification.

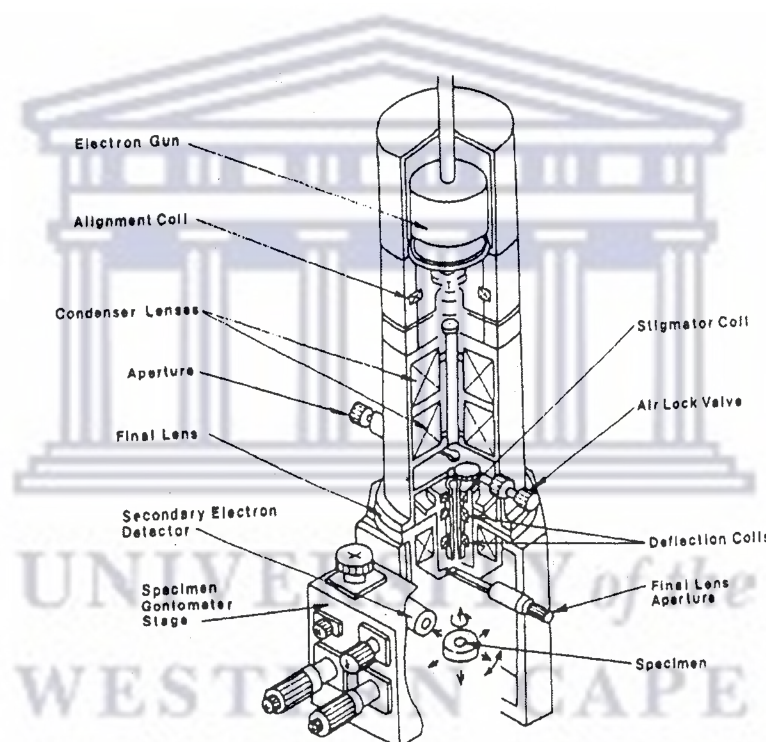

Fig 2.10 Schematic sketch of SEM.

The electron gun of a SEM is made up of a hair-pin shaped tungsten filament, Wehnelt cylinder and an anode plate. The electron gun and the Wehnelt cylinder are connected to the negative pole of high voltage supply, since filament is negatively charged, there is a potential difference established between the filament and the grounded anode plate. This will cause the electrons to accelerate towards the anode.

http://etd.uwc.ac.za/

As shown in the figure 2.10 the accelerated electrons pass through the aperture of the anode and down the condenser lenses causing the electrons to converge and pass through a focal point. The settings of the condenser lens are such that the focal point is above the condenser aperture. This condenser aperture trims off the nonhomogeneous and scattered electrons and only lets through the focused homogeneous beam of electrons. This beam of electrons diverges below the condenser lens aperture, where the final lens brings the beam into focus at the sample by demagnifying the beam of electrons to a focal point at the sample surface. This final lens demagnification determines the diameter of the electron beam on the sample.

When these electrons impinge the sample there are various signals that are produced, x-rays being one of them which is the characteristic of the elemental atom.

X-ray's emitted during EDS analyses of the sample were processed, this was done by an energy dispersion with a semiconductor detector. This ultimately will give an energy spectrum of the sample under investigation [37].

In the case of our sample, the area of interest was the border between the edge of the aluminium and the a-Si:H film. The sample was mounted on the sample holder with silver paste for increased conduction. Then the region of interest was analyzed by EDS for the presence of aluminium.

UNIVERSITY of the
WESTERN CAPE

http://etd.uwc.ac.za/

CHAPTER 3

RESULTS

3.1 INTRODUCTION

In this chapter we will present results of the experiments carried out during the investigation of the crystallization of a-Si:H using the aluminium induced crystallization (AIC) technique. The results will also answer the question of whether there is any crystallization growth laterally to the side not covered by aluminium.

The thickness of the aluminium films were measured by using a Dektak profilometer. A typical graph of the step heights of the measured values of these films will be presented in this chapter.

Energy dispersive spectroscopy (EDS) technique was employed to confirm that only the elements in the substrates and the deposited films are present in the samples and no other impurities were incorporated during the depositions. The spectra of this analysis will be given in this chapter.

The Rutherford backscattering spectrometry (RBS) spectra giving depth profiles of the diffused aluminium into the a-Si:H film are also presented, this will be used in explaining how the aluminium diffuses into the a-Si:H film at different annealing times and temperatures, and also in the determination of the depth of the diffused aluminium during the annealing. These spectra analyses were done using RUMP (Rutherford Universal Manipulation Program).

X-ray diffraction (XRD) analyses were also done for crystallinity studies for both the time and temperature series.

Transmission electron microscopy (TEM) was used to investigate whether there is any crystallization taking place laterally into the a-Si:H film not covered with aluminium.

http://etd.uwc.ac.za/

3.2 EXPERIMENTAL RESULTS

3.2.1 Thickness Measurement

A-Si:H thin films half covered by a layer of aluminium were analyzed using a Dektak profilometer to determine the thickness of the aluminium layer. The samples were placed on the profilometer sample stage and measured. The following typical trace was obtained from profiling.

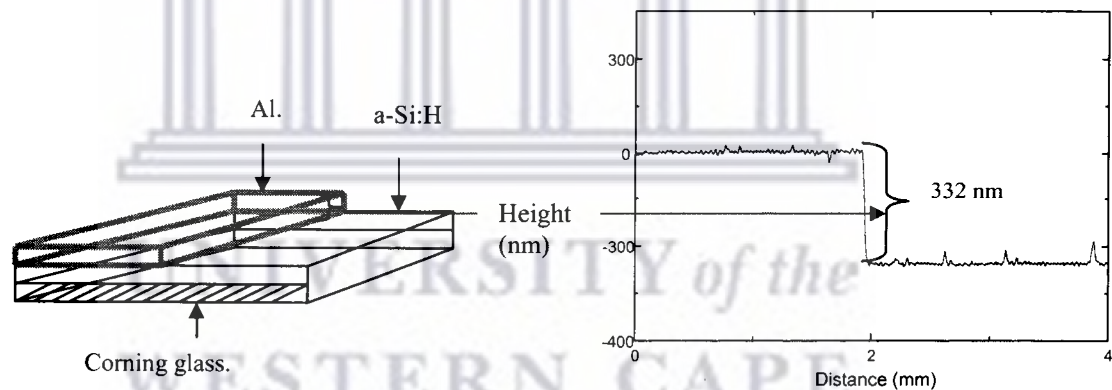

Figure 3.1 The graph of the thickness measurement of the aluminium layer.

Figure 3.1 show a graph plotted by the profilometer, the thickness of the aluminium layer was found to be 332 nm, and this was the layer for the time series. For the temperature series the thickness was the same.

http://etd.uwc.ac.za/

3.2.2 ENERGY DISPERSIVE SPECTROSCOPY (EDS)

Energy dispersive spectroscopy was used for elemental identification of the constituent elements as a means of confirming that only the substrates elements, silicon and aluminium were present in the samples. It was also used to investigate whether there was any lateral diffusion of aluminium to the uncovered a-Si:H layer during annealing.

The analysis was performed on the aluminium covered side and on the edge of the aluminium film where the a-Si:H film continues.

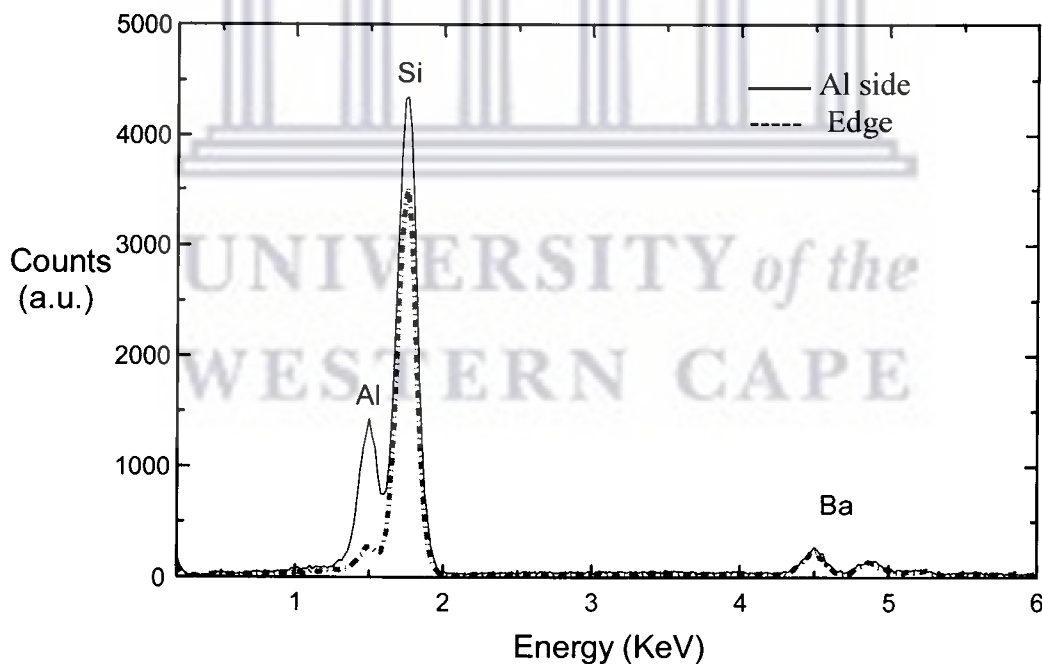

Figure 3.2 EDS spectrum of the Al side and at the edge.

The spectrum in figure 3.2 confirms the presence of aluminium, silicon and the substrate elements. At the edge of aluminium and where a-Si:H film continues there was no significant diffusion of aluminium during annealing, the hump at the

http://etd.uwc.ac.za/

aluminium energy at the edge is due to the Corning glass. (see appendix for the corning glass composition) The barium peak is also from the substrate material.

3.2.3 Rutherford Backscattering Spectrometry (RBS).

The Rutherford backscattering technique was used for depth profiling of aluminium into the a-Si:H matrix before and after annealing. During annealing of the samples aluminium diffuses into the a-Si:H matrix hence migrating from the top surface into the a-Si:H matrix.

The spectra in figures 3.3.a and 3.3b depict the schematic of migration of aluminium into the a-Si:H matrix during the annealing process.

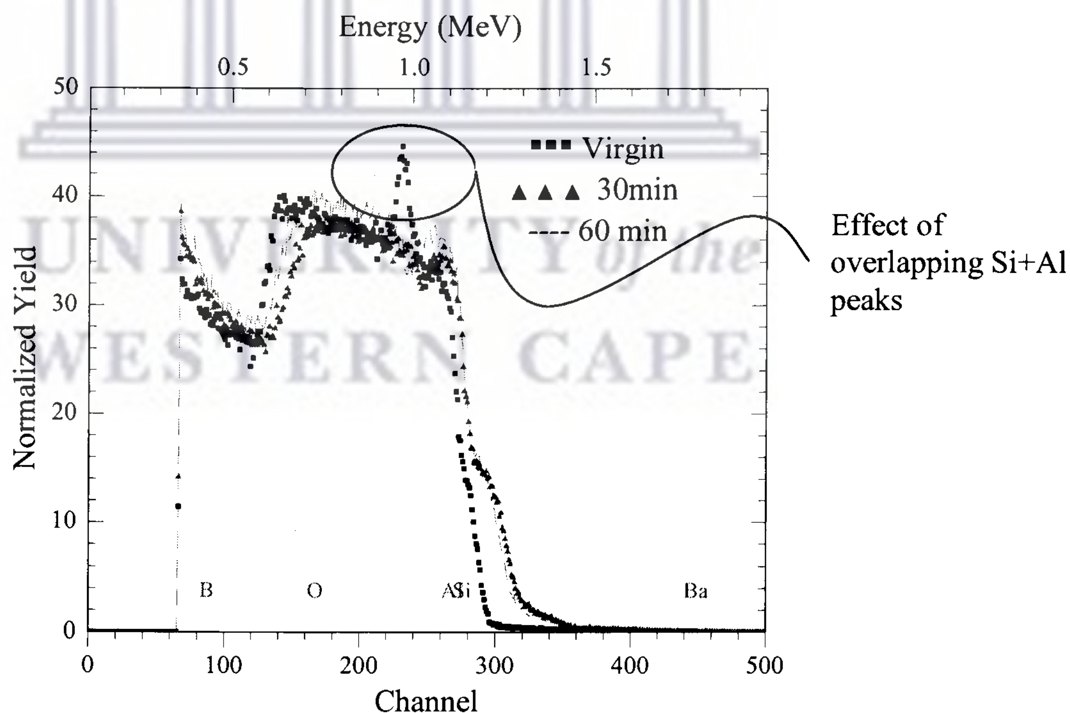

Figure 3.3a RBS spectrum of the time series up to 60 minutes annealing.

http://etd.uwc.ac.za/

The peak seen on the virgin sample is due to the overlapping of aluminium at the surface and silicon in the next layer. As the samples are annealed, aluminium diffused into the a-Si:H matrix, hence the diminishing of the peak .

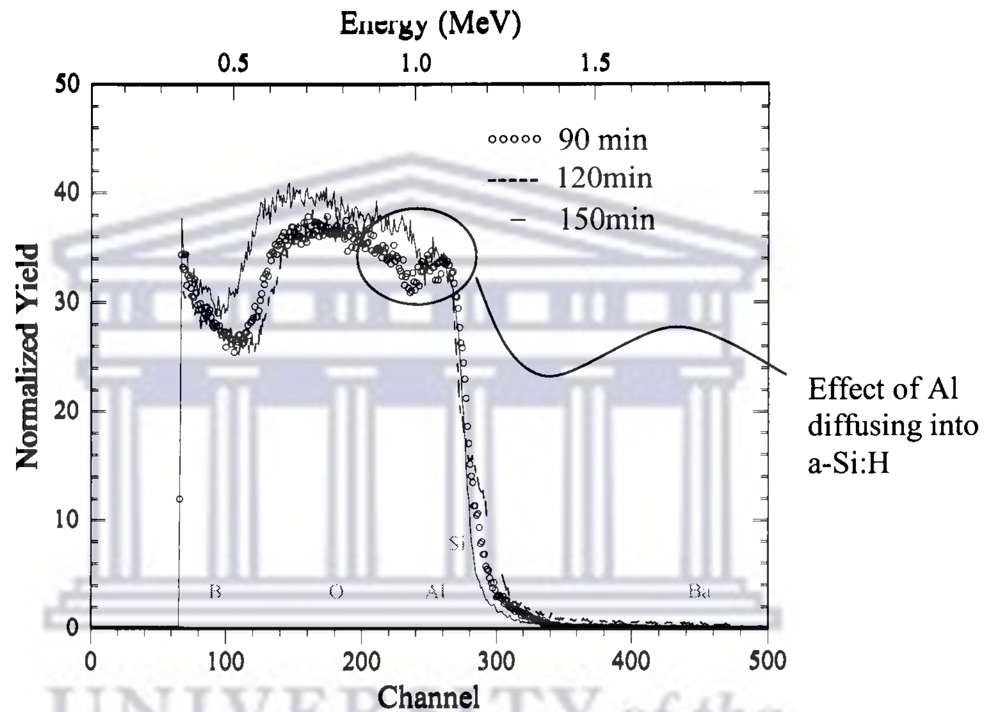

Figure 3.3b RBS spectrum of the time series beyond 90 minutes annealing.

The aluminium that diffused into the a-Si:H film induces crystallization by enhancing the rearrangement of the a-Si:H network, and it also reduces the activation energy of the a-Si:H dissociation [39]. This aluminium also acts as nucleation sites for the growth of poly C-Si [40]. The table 4 presents the surface density amount of diffused aluminium in the a-Si:H.

http://etd.uwc.ac.za/

Table: 4 RBS data of diffused aluminium.

Temperature [°C]	Annealing duration [minutes]	Aluminium on top [atoms/cm^2]*	Aluminium diffused [atoms/cm^2]*
450°C	0	2000	0
	30	1500	500
	60	1500	500
	90	1500	500
	120	1500	500
	150	1500	500

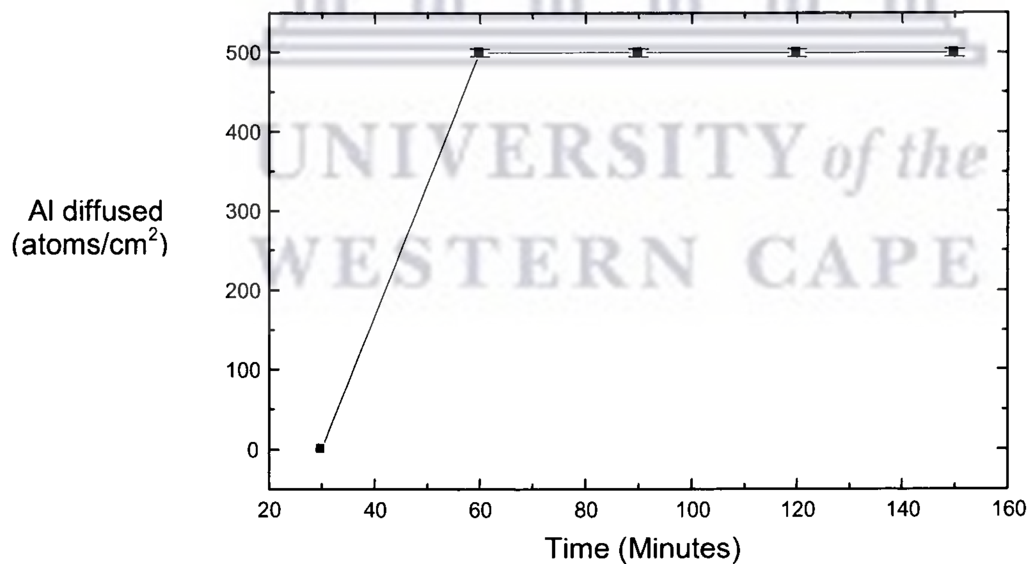

Figure 3.4 The graph of diffused aluminium v/s annealing time.

From the graph in figure 3.4 it is evident that after the initial diffusion time of 30 minutes no further diffusion occurs of aluminium into the a-Si:H film.

http://etd.uwc.ac.za/

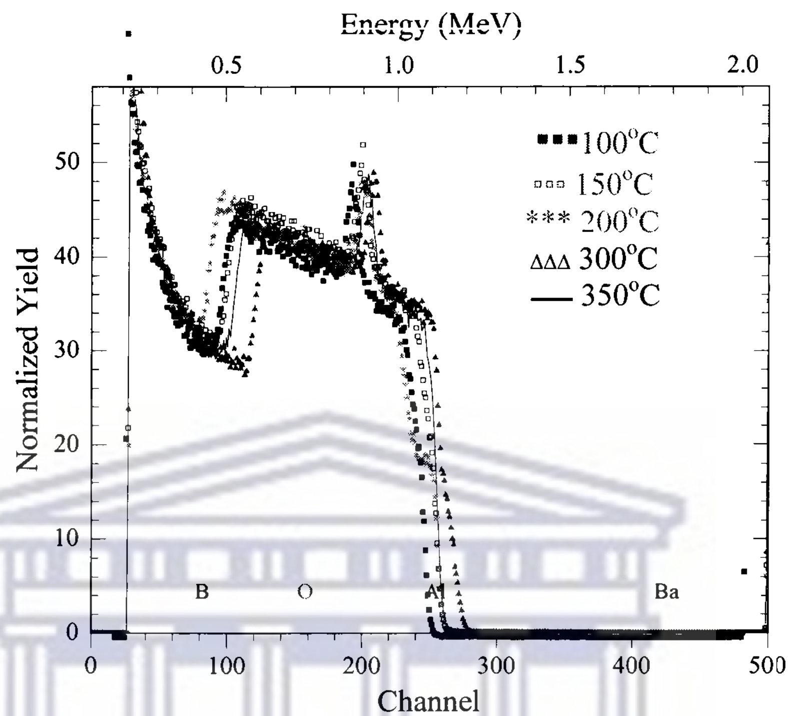

Fig 3.5 RBS Spectra of the temperature series

For the RBS temperature series spectra in figure 3.5 it is clear that there is no aluminium diffusion from the top aluminium layer into the a-Si:H film. The aluminium layer remains essentially at the same thickness at all temperatures, leading to the assumption that no aluminium diffusion into the a-Si:H layer took place. Hence from the temperature series samples no crystallization is expected.

3.2.4 X-ray DIFFRACTION (XRD)

Crystallinity studies were done on the as-deposited and on the annealed samples using the Bruker Advanced θ - 2θ XRD machine at iThemba LABS. This was done on the two classes of samples processed (i.e. temperature series and time series) as tabulated in tables 2 and table 3, the samples were analyzed on the alumunium covered side using the same set of conditions. Figure 3.7a and 3.7b shows the spectra of the time series (i.e. annealed at 450°C for varying minutes).

http://etd.uwc.ac.za/

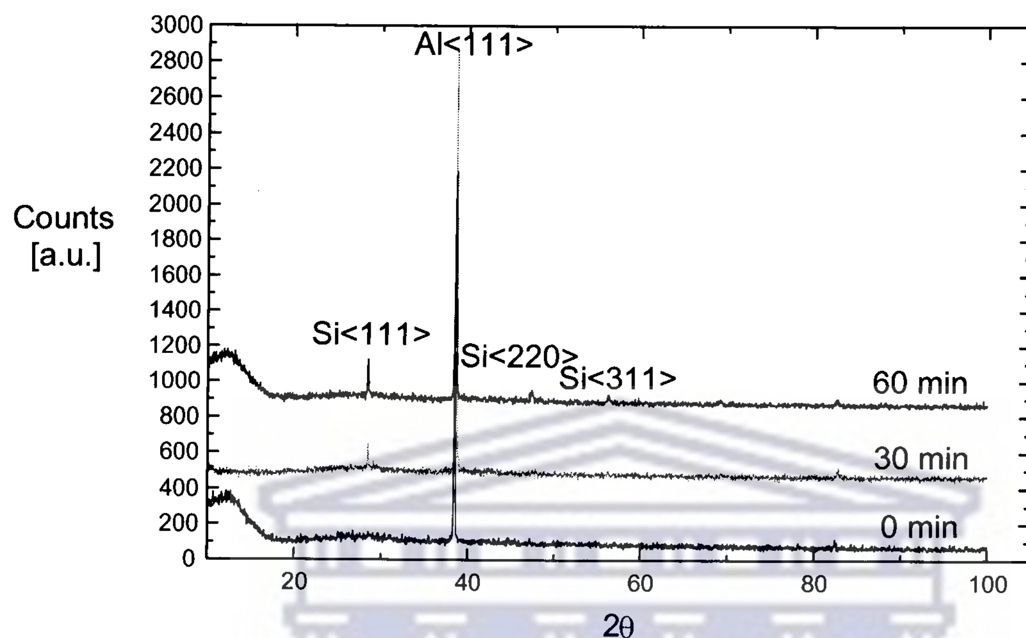

Figure 3.7a The XRD spectra of the annealing time series up to 60 min

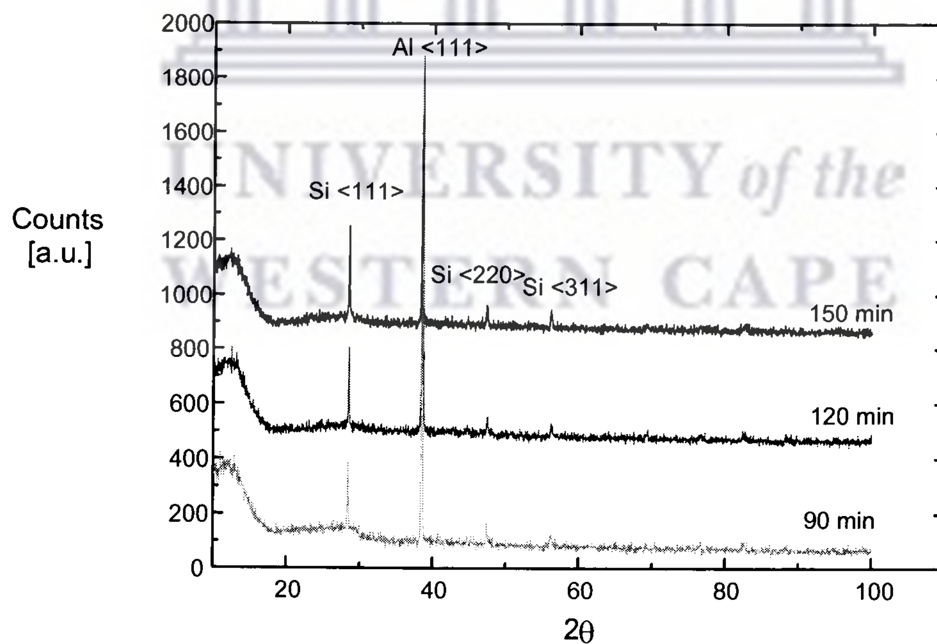

Figure 3.7b The XRD spectra of the annealing time series annealing beyond 90 min

http://etd.uwc.ac.za/

The Si<111> peaks at 28.1° show a trend of increasing intensity with the annealing time. The preferred Si<111> orientation for poly C-Si was used since it is more intense compared to Si<220> at 47.3° and Si<311> 56.4°.

Table 5 of Annealing time series.

Temperature[°C]	Time [minutes]	Counts c-Si<111>	Relative to 30 min peak
450°C	0 min	0	0
	30 min	261	1
	60 min	330	1.26
	90 min	359	1.38
	120 min	412	1.58
	150 min	467	1.79

The tabulated results in table 5 are extracted from these series of spectra. From the graph of this data in figure 3.8 it is evident that the crystallinity of the annealed sample increases with time. It should be borne in mind that from the RBS analysis in table 4 and the RBS spectra, the amount of diffused aluminium is observed to be the same for all crystallized sample. From the XRD spectra in figure 3.7a and 3.7b of the time series it is concluded that crystallinity of the poly c-Si increases with increasing annealing time.

http://etd.uwc.ac.za/

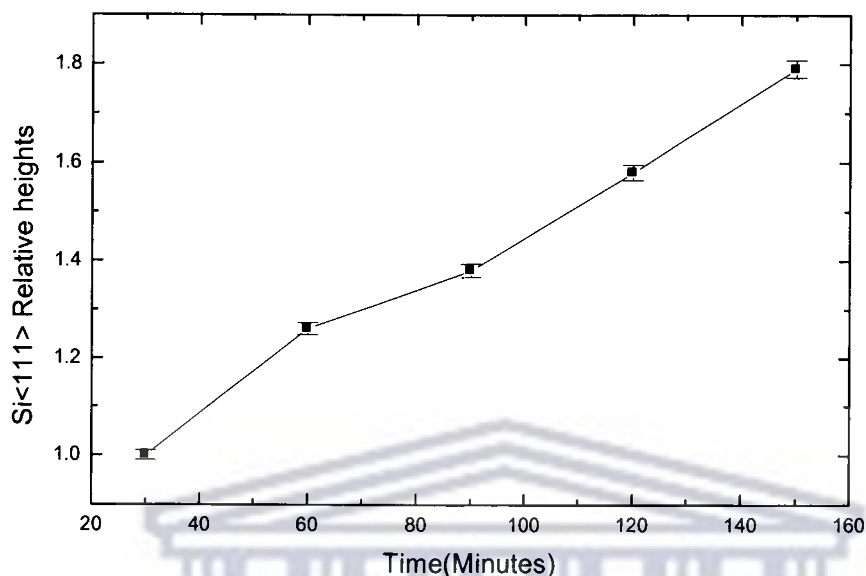

Figure 3.8 The graph of relative peak heights of Si<111> v/s annealing time.

The XRD spectra were also measured on the temperature series samples, as shown in figure 3.9. A 25° to 42° scan range was done on temperature series samples, because Si<111> and Al<111> peaks of interest are within that range.

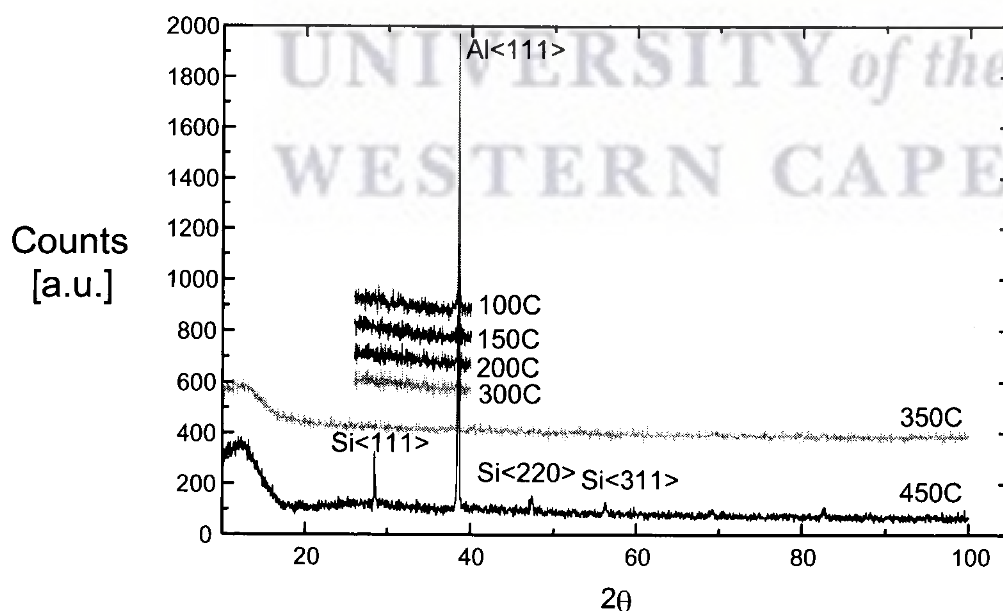

Figure 3.9 The XRD spectra of the temperature series.

http://etd.uwc.ac.za/

The temperature series XRD spectra in figure 3.9 shows no evidence of crystallinity from the XRD spectrums until the 450°C spectrum when the Si<111> peak appeared.

3.2.5 Transmission Electron Microscopy (TEM)

Since the objective of this investigation was to determine whether there is lateral crystallization of the a-Si:H layer across from the aluminium covered side into the uncovered side, this made it necessary to investigate what happens at the edge between the uncovered side and the covered side.

From the TEM micrograph in figure 3.10 the arrow points at the deposited aluminium layer edge and where the original a-Si:H film continues. From the micrograph it can be seen that the a-Si:H material crystallized below the aluminium film, and then some lateral crystallization appears away from the aluminium edge. The remaining uncrystallized a-Si:H layer is visible beyond this lateral crystallization growth region.

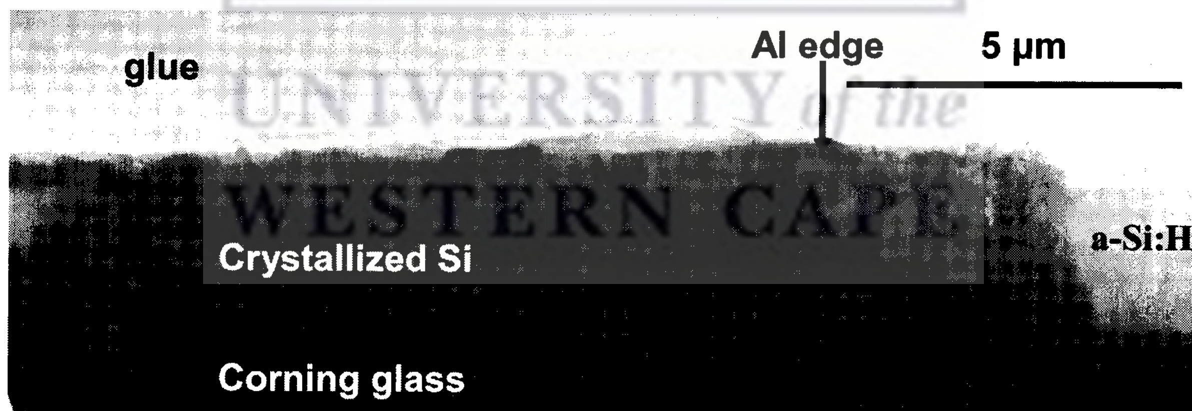

Figure 3.10 TEM micrograph of the aluminium edge.

In figure 3.11 a SAD patterns of the poly c-Si gives a further proof that the original a-Si:H film under the aluminium layer is crystallized, and lateral growth of crystallization has occurred which is evident from the continuous similar texture of the poly c-Si beyond the aluminium edge.

http://etd.uwc.ac.za/

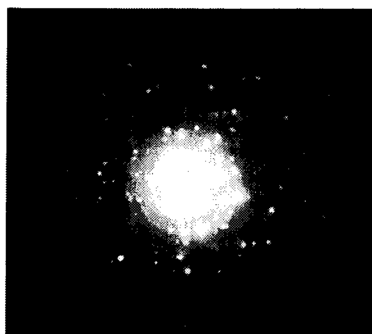

Figure 3.11 SAD patterns of poly c-Si.

Also in figure 3.12 the SAD patterns of the uncrystallized a-Si:H region of the film, beyond the lateral crystallized growth region shows that the region is indeed amorphous.

UNIVERSITY of the
WESTERN CAPE

Figure 3.12 TED image of a-Si:H

From the TEM micrograph in figure 3.10 visual inspection shows that the amorphous region looks different from the crystalline region in texture, therefore a conclusion can be safely drawn that indeed the few micro-meters of silicon film beyond the aluminium edge is indeed crystallized.

http://etd.uwc.ac.za/

CHAPTER 4

DISCUSSION

4.1 INTRODUCTION

In this work an investigation of crystallization of thin films of a-Si:H using the AIC technique was carried out. The amount of aluminium diffused into the a-Si:H film was determined using RBS, this diffused amount of aluminium was compared to the diffraction peaks intensity from the XRD spectrums for the time series samples. The results of the investigation showed that after 500×10^{15} atoms/cm^2 of aluminium have diffused into the a-Si:H film crystallization was induced. No further diffusion of aluminium took place as was concluded from the RBS simulations, but on the other hand the crystallinity of the samples improved with annealing time as it was evident from the peak heights of the XRD spectra. These XRD measurements were done under the same conditions except for the temperature series in which the scan range was from the 25^0 to 42^0 region of interest.

The results collected during this work showed that minimum times and lower temperature can be used to crystallize a-Si:H covered with aluminium layer, compared to solid phase crystallization of a-Si:H deposited on Corning 7059 glass.

UNIVERSITY of the
WESTERN CAPE

4.2 ANALYSIS OF RESULTS

The reason for these minimum times and lower temperatures to induce crystallization is the presence of the aluminium layer on top of a-Si:H film during annealing. According to the nucleation and growth mechanism, crystallization occurs by nucleation followed by growth [40] of the a-Si:H. Aluminium diffusing into the a-Si:H film acts as nucleation sites, and further growth to poly c-Si occurs from those sites [41]. From figure 3.10 it can be clearly seen where the aluminium edge is, and where the original a-Si:H continues. There are two possible processes that can cause aluminium to migrate from the aluminium edge to the region beyond

http://etd.uwc.ac.za/

The first is surface melting of the aluminium. For surface melting of aluminium to take place temperatures of approximately 660°C [42] have to be reached, and from the experiments the highest temperature reached was 450°C. It can thus be safely concluded that surface melting of aluminium did not take place.

The second factor that can cause aluminium to migrate from the edge to the region beyond is by diffusion of aluminium from the overlaid side to the uncovered side. From the EDS results in figure 3.2 there is an aluminium hump from the analysis at the edge of aluminium where the original a-Si:H film continues. This hump is due to the contribution of the traces of aluminium from the corning glass substrate as stated in its composition in the appendix. It should be mentioned that these traces of aluminium from the corning glass have no ability whatsoever to induce crystallization as it is bonded as an oxide. It also is evident from the a-Si:H side beyond the lateral crystallization growth in figure 3.10, where no signs of crystallization is shown and also from the SAD patterns in figure3.12.

Experiments done by other research groups on solid phase crystallization of a-Si:H films on corning glass show no evidence of crystallization induced by these aluminium traces from the Corning 7059 glass substrate [43]. On the other hand the hump at the aluminium energy peak in figure 3.2 could be from the diffused aluminium from the edge. If this was the case that aluminium would not have been enough to induce any meaningful crystallization, since it would be below the minimum required aluminium to induce any meaningful crystallization as evident from figure 3.2 EDS spectrum [44] .

The process of crystallization due to the aluminium layer starts to happen at the temperature of about 450°C, at temperatures lower than that no diffusion of aluminium has taken place shown in figure 3.6, hence no nucleation sites for silicon was created. This is clearly seen from the XRD spectra in figure 3.9 that shows the contribution of the amorphous silicon hump and no silicon crystalline peaks.

http://etd.uwc.ac.za/

At the beginning of crystallization the silicon nuclei centers grow in all directions [45], this happens until all the a-Si:H overlaid by aluminium has transformed into poly c-Si during annealing. As the nuclei grows in all directions, the nuclei formed at the edge of the aluminium layer where the a-Si:H film is not covered by aluminium continues also to grow in all direction, including the lateral direction of the uncovered a-Si:H thin film. This growth continues until it encounters some stopping mechanisms from the a-Si:H thin film.

During the deposition process of the a-Si:H films, columnar growth occurs, leaving some small cracks between growing columns [43]. These cracks are visible from figure 4.1on the a-Si:H side of the sample.

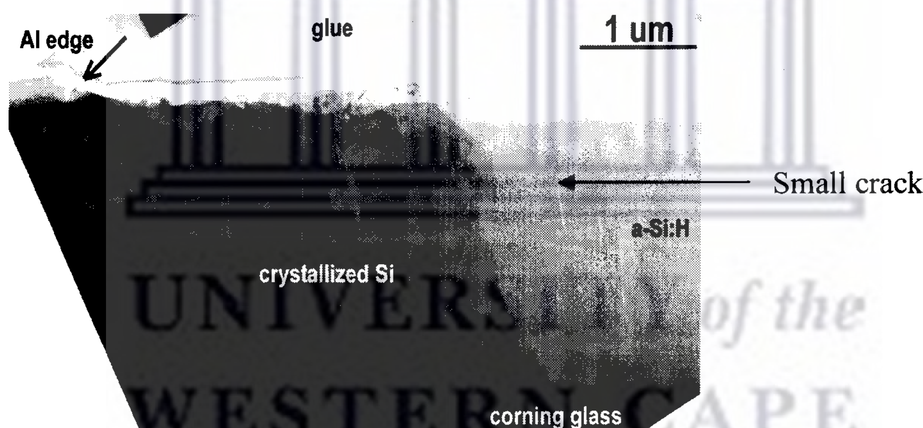

Figure 4.1 Lateral crystallized edge

It is proposed that these cracks then acts as stopping mechanisms that impair further growth of these nuclei of poly c-Si from the aluminium overlaid side to beyond the aluminium edge. This is evident from the distance of the lateral crystallization on the a-Si:H side as it only laterally crystallized up to approximately 2.5μm.

http://etd.uwc.ac.za/

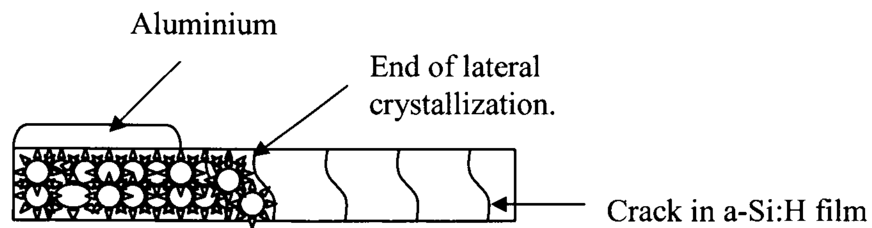

Figure 4.2 Schematics of lateral crystallization.

The TEM micrograph in figure 3.10 clearly showed this lateral crystallization beyond the aluminium edge. SAD patterns in figure 3.11 clearly shows the diffraction spots of the aluminium covered side, the visible crystallization of the aluminium covered side is the same as that of the laterally crystallized one, hence it can be concluded that indeed lateral crystallization has taken place.

UNIVERSITY of the
WESTERN CAPE

http://etd.uwc.ac.za/

CHAPTER 5

CONCLUSIONS

- Aluminium induced crystallization (AIC) of a-Si:H thin films was tested in this study as a technique that induces crystallization at lower temperatures and shorter processing times. Temperatures of 450°C for varying times were investigated and also temperature series studies were carried out on these samples.

- From the XRD spectra and RBS spectra simulation, it was evident that the crystallinity of the poly c-Si improves with annealing time as it was deduced from the XRD peak intensities. This implied that the Si<111> plane became a preferred orientation with annealing time.

- This work was then taken further to study the lateral crystallization of the a-Si:H film at the edge were aluminium layer ends. The uncovered a-Si:H film was crystallized due to the crystallization of the aluminium covered part, and this crystallization continued for approximately 2.5 μm away from the edge of aluminium layer.

- TEM and TED confirmed the crystallinity of the aluminium covered layer and also the lateral crystallized part of the sample. The diffused ring from of the TED showed that the a-Si:H film not covered by aluminium beyond the lateral crystallized growth of the original a-Si:H at the aluminium edge was not crystallized during the annealing process, which is more proof that the crystallization of the aluminium covered part was due to aluminium not solid phase crystallization.

http://etd.uwc.ac.za/

- Lateral crystallization looks promising as a way of using minimum metal layer to induce crystallization of the a-Si:H films. It is proposed that if more dense and less cracks and microvoid a-Si:H film can be prepared. Longer lateral crystallization distances can be achieved.

http://etd.uwc.ac.za/

CHAPTER 6

FUTURE WORK

- Quantification of hydrogen content using Elastic recoil Detector ERD and Fourier Transform Infra Red (FTIR).
- Minimum aluminium thickness to induce crystallization of a-Si:H.
- Influence of the aluminium thickness on lateral crystallization.
- RBS channeling to determine the crystallinity of the crystallized layer.
- The role of hydrogen in the lateral crystallization.

UNIVERSITY of the
WESTERN CAPE

http://etd.uwc.ac.za/

REFERECES

[1] M.A. Green, Solar Cell – Operating Principles, Technology and System Applications, Prentice-Hall, New Jersey (1982)

[2] T. Markvart, Solar Electricity. John Wiley & Sons, Chichester (2000)

[3] Y. Masaki, P.G. Lecomber, and A.G. Fitzgerald, J. Appl .Phys. 74, 1 (1993)

[4] David Adler, Brain B. Schwartz, Martin C. Steele, Physical Properties of Amorphous Meterial. 45-48

[5] P. delli Veneri, C.Privato, E. Terzini. J. Non-Crysta Solids 266-269, 635-639 (2000)

[6] T. Matsuyama, N. Terada, T Baba, T. Swada, S. Tsuge, K. Wakisawa, S. Tsuda, J. Non-Cryst. Solids 198-200, 940 (1996)

[7] J.S. Im, R.S. Sposili, M.A. Crowder, Appl. Phys. Lett. 70, 3434 (1997)

[8] Y.H. Zhao, J.Y. Wang, E.J. Mittemeijer, Thin Solid Films 433, 82-87 (2003)

[9] B.Y. Tsaur and Suzaki, J.W. Mayer, Philos. Mag. A43, 345 (1981)

[10] S.R. Herd, K.Y. and K.N. Tu, Thin Solid Films 104, 197 (1983)

[11] K. Yoshi, Y. Suzaki, A. Takeuchi, K. Yasutake, and H. Kawabe, Thin Solid Film 199, 85 (1991)

[12] M. Morimotom A Kumeda, and T Shimuzi, J. Non-Cryst. Solid 59&60, 537 (1983)

http://etd.uwc.ac.za/

[13] H. Suto and H. Ishikawa, Trans. Jpn. Ins. Met 17, 596 (1976)

[14] T. Lucinski and J. Baszynski, Phys. Status solid A 84, 607 (1984)

[15] H. Nasu, M. Watanabe, K Shizuma, S. Makida, M. Ueda, T. Imura, Y. Osaka, and H. Hassi, J. Non-Cryst. Solids 95&96, 5663 (1987)

[16] E. Nygren. J.S. Williams, R.G. Elliman, A.P. Pogay, G.L. Olson and J.C. McCallum, Proceedings of the Material Research Society Symposium (MRS, Pittsburg, P.A, 1987) Vol.74, p307

[17] E.Nygren, A.P. Pogany, K.T. Short, J.S. Williams, R.G. Elliman, and J.M. Poate, Apl.Phys.Lett. 52, 439 (1988)

[18] D.C. Booth D.D. Allred, and B.O. Seraphin, J. Non-Cryst. Solid 35&36, 213 (1980)

[19] A. Mrimoto , T. Kataoko, M. Kumeda, and T. Shimuzu, Philos. Mag. B 50, 517 (1984)

[20] B. Andersson, Ph.D. thesis, ISDN: 91-7372-523-4, Linkoping University (1982)

[21] I. Grimberg, B.Z. Wiess, and S.R. Herd, Acta Metall. 37, 2475 (1981)

[22] C.A. Hewett, I. Suni, L.S. Hung, and S.S. Lau, in Layered Structures and Interface Kinetics, edited by S Furukawa (KTK Scientific, Tokyo, 1985).

[23] S.R. Herd, I.M. Fisher, G.U. Singco, R.D. Thompson, and K.N. Tu, Matr. Chem. Phys. 34, 3 (1993)

http://etd.uwc.ac.za/

[24] M. Vernat, G. Marchal, P. Mangin, 14th International conference on Amorphous Semiconductors Science and Technology, 1991, edited by G.H. Bauer, W. Fuhs, and L. Ley (North Holland, Amsterdam, 1991), Vol.1 p1923

[25] K. Akitmoto and K. Watanabe, Appl. Phys. Lett 39, 445 (1981)

[26] T. Ohnishi, N. Yokoyama, H. Onodera, S. Suzuki and A Shibatomi, Appl. Phys. Lett. 43, 600 (1983)

[27] R.E. Thomas, J.H. Perpepezko, and J.D. Wiley, Appl. Spectrosc. 26 , 534 (1986)

[28] G Liu, S.J. Fonash, Appl. Phys. Lett. 62, 2554 (1993)

[29] C.Y. Yuen, M.C. Poon, W.Y. Chan, J .Appl. Phys. 92, 6291 (2002)

[30] S.W. Lee, Y.C. Jeon, S.K. Joon. Apply. Phys. Lett 66, 913 (1995)

[31] M.S. Ashtika, G.L. Sharma, J. Appl. Phys. 78, 913 (1995)

[32] O. Nast, T. Puzzer, L.M. Koschier, A.B. Sproul, S.R. Wenham, Appl. Phys. Lett. 73, 314 (1998)

[33] O. Nast, S Brehme, S. Pitchard, A.G. Aberle, S.R. Wenham, Sol.Energy Mater. Sol. Cell (2001) 385

[34] I. Gordon, D. Van Gestel, K. Van Nieuwenhuysen, L. Carnel, G. Beaucarne, J. Poortmans. Thin solid Films 487, 113-117 (2005)

[35] Dektak 6M Manual Vecco p6 section 1.4

UNIVERSITY of the WESTERN CAPE

http://etd.uwc.ac.za/

[36] W.K. Chu, J.W. Mayer, and M.A. Nicolet, Backscattering Spectrocsopy (Academic Press, New York, 1978)

[37] T. Michael, Postek, Jr and Ladd Research Industries, Inc Scanning Electron Microscopy, a student's handbook, (1980)

[38] R. Rao, G.C Sun, J. of Crys. Growth. 273 68-73 (2004)

[39] S. Gall, M. Muske, I. Sieber O. Nast W. Fuhs. J of Crys. Solids. 299-302 (2002)

[40] R. Rao, G.C Sun, J. of Crys. Growth. 273 68-73 (2004)

[41] S. Gall, M. Muske, I. Sieber O. Nast W. Fuhs. J of Crys. Solids. 299-302 (2002)

[42] www.webelements.com

[43] Chan-Do Park, Hae-Yeol Kim, Min-Hee Cho, Kuk-Jin Jan, Jai-Young Lee, Thin Solid Film. 268-274

[44] G.J. Qi, S. Zhang, T.T. Tang, J.F. Li, X.W. Sun, X.T. Zeng, Surface and Coating Technology. 198 300-303. (2005)

[45] Abbie Liebman Product Line Manager, Thin Sheet Glass & Refractories
liebmanas@corning.com

UNIVERSITY of the
WESTERN CAPE

http://etd.uwc.ac.za/